Agronomy Research **17**(2), 349–357, 2019
https://doi.org/10.15159/AR.19.119

RGB vegetation indices applied to grass monitoring: a qualitative analysis

B.D.S. Barbosa[1], G.A.S. Ferraz[1], L.M. Gonçalves[1], D.B. Marin[1], D.T. Maciel[1], P.F.P. Ferraz[1] and G. Rossi[2]

[1]University Federal of Lavras, Department of Engineering, Federal University of Lavras, BR37200-000 Lavras-Minas Gerais, Brasil
[2]University of Florence Studies, Department of Agricultural, Food, Environment and Forestry (DAGRI), Via San Bonaventura, 13, IT50145 Firenze, Italia
[*]Correspondence: gabriel.ferraz@ufla.br

Abstract. In developing countries such as Brazil, research on low-cost remote sensing and computational techniques become essential for the development of precision agriculture (PA), and improving the quality of the agricultural products. Faced with the scenario of increasing production of emerald grass (Zoysia Japônica) in Brazil, and the value added the quality of this agricultural product. The objective of this work was to evaluate the performance of RGB (IV) vegetation indices in the identification of exposed soil and vegetation. The study was developed in an irrigated area of 58 ha cultivated with emerald grass at Bom Sucesso, Minas Gerais, Brazil. The images were obtained by a RGB digital camera coupled to an remotely piloted aircraft. The flight plan was setup to take overlapping images of 70% and the aircraft speed was 10 m s^{-1}. Six RGB Vegetation index (MGVRI, GLI, RGBVI, MPRI, VEG, ExG) were evaluated in a mosaic resulting from the images of the study area. All of the VIs evaluated were affected by the variability of lighting conditions in the area but MPRI and MGVRI were the ones that presented the best results in a qualitative evaluation regarding the discrimination of vegetation and soil.

Key words: ARP, emerald grass, index vegetation RGB.

INTRODUCTION

The increasing demand for grass and for higher-quality grass by the consumer market is responsible for the increased grass production area in Brazil, especially in locations near large consumer centres (Godoy et al., 2012). Given the increased demand, the monitoring of this crop is extremely important and is viable using precision agriculture (PA) techniques. In developing countries, the use of remote sensing techniques with low financial and computational costs has become essential for the development of small agricultural businesses (Ponti, 2013) and generates higher profitability for the agricultural enterprise.

For the success of PA, the use of remotely piloted aircraft (RPA) has increasing potential for agricultural monitoring by obtaining data with remote sensing techniques. The advantages of RPA include lower acquisition costs than other platforms for obtaining aerial data, flight speeds that are suitable for collecting aerial data, high spatial resolution, and low risk of accidents involving human operators (Xiang & Tian, 2011; Vega et al., 2015).

In agricultural research, the use of conventional consumer cameras has increased due to the low acquisition cost, but the potential and costs of this branch of agricultural research requires further studies (Zhang et al., 2016).

Consumer cameras on aircraft have been used for several applications in agricultural monitoring, including forage yield prediction (Hunt et al., 2013), plant detection (Barrero & Perdomo, 2018), agricultural pest monitoring (Yang & Hoffman, 2015), and green vegetation distinction (Romeo et al., 2013; Kazmin et al., 2015). Cameras are already being used for crop monitoring and protection by several farmers with high levels of technology deployed on their properties (Zhang et al., 2016).

One way to better identify changes in agricultural fields is to use a vegetation index (VI) (Xiao & Moody, 2005). To determine the effect of UV radiation on the vegetation canopy, MRI is determined by the electromagnetic radiation (EMR) reflected by vegetation canopies that is detected by the passive optical sensor, but the reflected REM varies according to the chemical and structural structure of each species (Liu et al., 2016; Zhang & Kovacs, 2012). In the case of a conventional camera, REM is detected in the portion of the visible in the electromagnetic spectrum (Red-R, Blue-B and Green-G), more commonly to evaluate characteristics such as the nutritional state of the plant (Vergara-Diaz et al., 2016). VIs are also used in the management of agricultural practices, mainly in crops of high economic value and with high production costs (Hamuda et al., 2016), benefiting farmers with cost reduction in different agricultural operations.

Meyer & Neto (2018) emphasize the importance of research into developing a highly effective VI for distinguishing biomass, soil, and residues (e.g., straw, twigs, dried leaves), which can improve automated remote sensing applications, machine learning, plantation monitoring, and the application of precision farming techniques.

Several types of VIs are available in the literature; however, they are not efficient under non-uniform lighting conditions (Romeo et al., 2013).

Thus, the objective of this study was to analyse the behaviours of several VIs applied to images captured by a conventional RGB camera onboard a civil-use recreational RPA.

MATERIALS AND METHODS

Study site

The study was conducted in a grass (*Zoysia japonica*) cultivation area (Fig. 1), which covers a total of 58 ha. The area is irrigated by centre pivot irrigation equipment and is located in the municipality of Bom Sucesso, Minas Gerais (MG), Brazil (UTM 23K 509402.45 m E, 7662306.20 m s).

The planting of grass area is divided into 8 plots with different planting dates, which causes regions with different densities of vegetation as shown in Fig. 1, c.

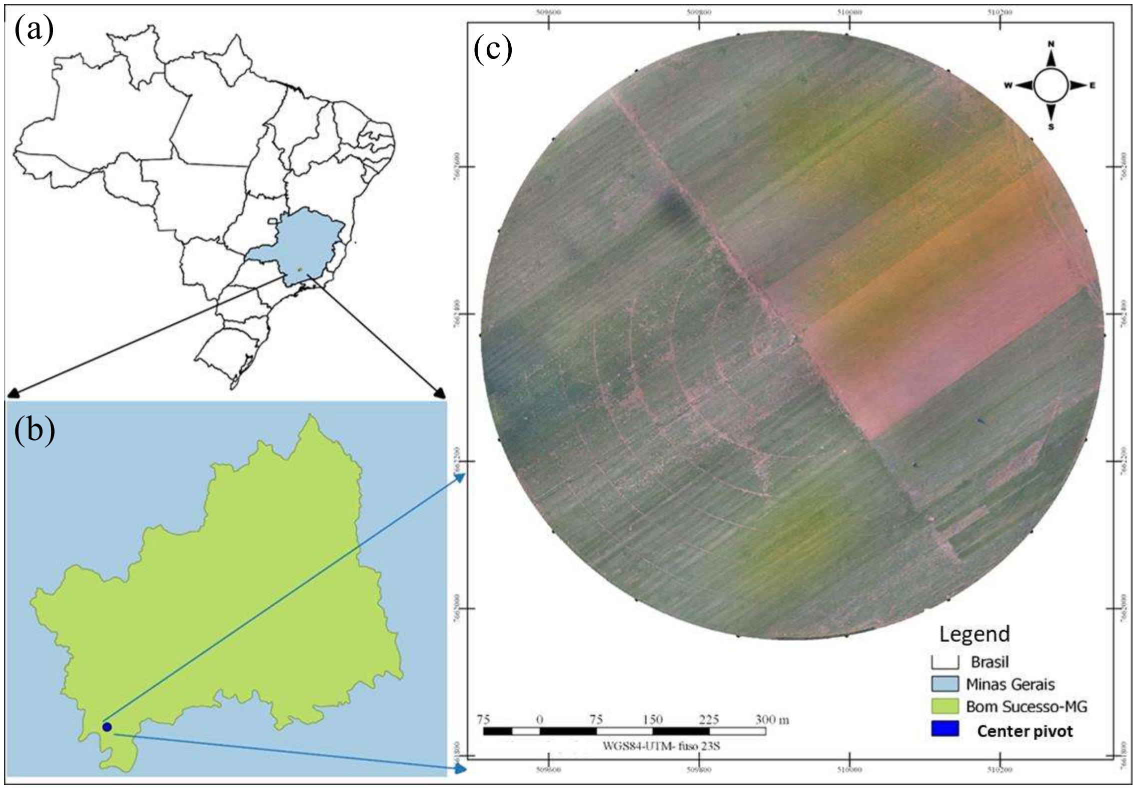

Figure 1. Study site location. (a) Brazil; (b) City; (c) Field of study.

Acquisition of aerial images

The images used in this study were obtained using an RPA (Phantom 3, DJI, Shenzhen, China) equipped with a Sony EXMOR 1/2.3 camera with 12.76 megapixels, a 94° FOV, an f/2.8 optical aperture, and sensors that capture electromagnetic radiation in the RGB spectral bands. The camera was coupled to a gimbal to stabilize it while in flight. The images were stored on an SD card.

Flight planning was done using the free application DroneDeploy, which is available for smartphones. The flight parameters are calculated based on the sensor information and the desired final spatial resolution. A spatial resolution of 6 cm was adopted for this study. To achieve this resolution, a flight height of 110 m and an average flight speed of 10 m s^{-1} were adopted as the flight parameters for the entire mission, and 70% longitudinal and lateral image overlaps were used. Rasmussen et al. (2014) recommend a frontal overlap of at least 75% and a lateral overlap of 60% for orthomosaic construction to obtain RGB images with conventional cameras. However, Kakaes et al. (2015) report that there is no globally accepted standard on the best overlap of frontal and lateral images and that the definition depends on the target to be imaged. The image overlaps and flight speed used in this study were first defined based on the operational capability of the equipment (flight time) at 10 m s^{-1}.

The flight schedule was set to between 12:00 and 2:00 p.m. to obtain good lighting conditions, as recommended by Bater et al. (2011), who reported that the images of RGB cameras are strongly influenced by hourly, daily, and seasonal lighting changes.

Image processing

The collected images were sent via the internet for image seaming (mosaicing) using the free trial version of the online DroneDeploy platform (www.dronedeploy.com). This platform returns a final product to the user in GeoTIFF format (mosaic) representing the fusion of the obtained images of the study site.

This mosaic was imported into the free geographic information system (GIS) software Quantum GIS version 14.2 (QGIS Development Team, Open Source Geospatial Foundation), in which the raster calculator tool was used to calculate the VIs (Table 1). The VIs are the results of algebraic operations between the spectral R, G and B bands that make up the mosaic.

Table 1. Vegetation Indices used in the study

IV	Name	Equation	Reference
MGVRI	Modified Green Red Vegetation Index	$\frac{(G)^2-(R)^2}{(G)^2+(R)^2}$	Bendig, et al. (2015)
GLI	Green Leaf Index	$\frac{2G-R-B}{2G+R+B}$	Louhaichi, Borman & Johnson (2001)
MPRI	Modified Photochemical Reflectance Index	$\frac{G-R}{G+R}$	Yang et al. (2008)
RGVBI	Red Green Blue Vegetation Index	$\frac{G-(B*R)}{(G)^2+(B*R)}$	Bendig, et al.(2015)
ExG	Excess of green	$2G-R-B$	Woebbecke et al. (1995)
VEG	Vegetativen	$\frac{G}{(R)^{a^*}*B^{(1-a)}}$	Hague et al. (2006)

a* = constant with value of 0.667; B = blue, G = green, R = red.

RESULTS AND DISCUSSION

The RGB mosaic showed areas with cloud shading (shaded area) and with higher reflectance (Area with spots), demarcated by polygons in the images (Fig. 2, A). The values found for all VIs represent that the higher the number presented by the evaluated VI, the greater the presence of vegetation in a certain area (green coloration), and for the exposed soil, the observed values are smaller (red coloration).

Rasmussen et al. (2014) suggest that in order to avoid this undesirable effect on images obtained by RPAs, images should be acquired on completely cloudy days or when the angle of light incidence is the same as the orientation of the camera so that the lighting conditions are as as possible. Bannari et al. (2009) emphasizes that the IVs are subject to variations in their values due to several factors, mainly due to the presence of shadows, solar brightness and pixel mix, which does not reflect the real surface condition.

According to Rasmussen et al. (2014), mosaicing software can cause spots to be present due to changes in the light reflection angle; thus, several software packages should be tested to determine which is best for each VI to be applied. Faced with this problem, Ortega-Terol et al. (2017) developed software for flight planning, processing images acquired with RPAs, and detecting areas with changes in sunlight reflectance. Their analysis was successful, thus providing an additional tool for noise detection in orthomosaics.

Another factor that should be discussed and investigated is the thresholds of the flight planning parameters that must be adopted to obtain the images. In this study, based on flight safety concerns, frontal, and lateral overlaps of 70% were adopted initially due to the limitations of the available flight time, which may have affected the quality of the generated mosaic. According to Torres-Sánchez et al. (2018), the definition of better overlap rates between images requires further study because this definition affects both the flight time and the processing time of the images.

According to Feng et al. (2015), processing aerial images obtained by RPAs, including orthorectification and image seaming, is not a trivial task due to the large number of images obtained, which have different characteristics, such as variations in lighting conditions.

All VI evaluated were probably affected by the solar reflection angle (area with spots), which was not evaluated in this study, or by the presence of shadows (Shaded area). Among the VI studied, the modified photochemical reflectance index (MPRI) had a smaller effect of yellow spots on the image (Area with spots)

MPRI can be inferred as the most adequate index to evaluate vegetation variability and soil cover, since it provided the best visual distinction between these variables. However, in the upper left portion of Fig. 2, B, MPRI is affected by cloud shading (indicated by arrows). This interference by means of shadows can lead the producer to believe that the vegetation present in these areas is at a higher stage of development than in neighboring areas, ready for harvest. This type of information can lead to erroneous crop management decisions and can lead to economic losses.

Ortega-Terol et al. (2017) point out that in multispectral images in which the normalized difference vegetation index (NDVI) is applied, errors of approximately 20% in the prediction of the VI values may compromise decision-making on crop management, irrigation planning, and other agricultural practices. These authors emphasize that when areas affected by variations in sunlight reflectance are identified, they should be eliminated from agronomic analysis when VIs are applied for vegetation analysis.

GLI (Fig. 2, C) had an inverse behavior to that observed for MPRI. This VI was effective only in the identification of exposed soil (Red coloration), not being efficient in the vegetation enhancement. In regions with spots (indicated by arrows in Fig. 2, C) GLI presented high values ($GLI > 0.11$) indicating a higher vegetation cover in this region, which is not confirmed by the analysis presented in Fig. 2, a and by field analysis.

MGRVI (Fig. 2, D) also provided good results, being able to efficiently highlight vegetation and soil, with results close to results obtained visually by MPRI (Fig. 2, B). The factor of not being chosen in this study as the best performing LV is due to the fact that it is more affected by the shadows (indicated by the arrows in Fig. 2D) than MPRI. The MGRVI has potential for studies of agricultural productivity and, according to Bending et al. (2015), this VI is promising for the prediction of barley biomass. These authors encourage further studies on the behavior of this VI, especially in other cultures.

The red-green-blue vegetation index (RGBVI) (Fig. 2, E) had the same behavior of the excess of green (ExG) (Fig. 2, H) and GLI (Fig. 2, C), being qualitatively inferior to the results presented by the MPRI (Fig. 2B). The RGBVI shows a different behavior of the vegetation in areas with the presence of yellow spots indicated with arrows in Fig. 2, E, in comparison with the MPRI and Fig. 2, A, showing a higher density of vegetation.

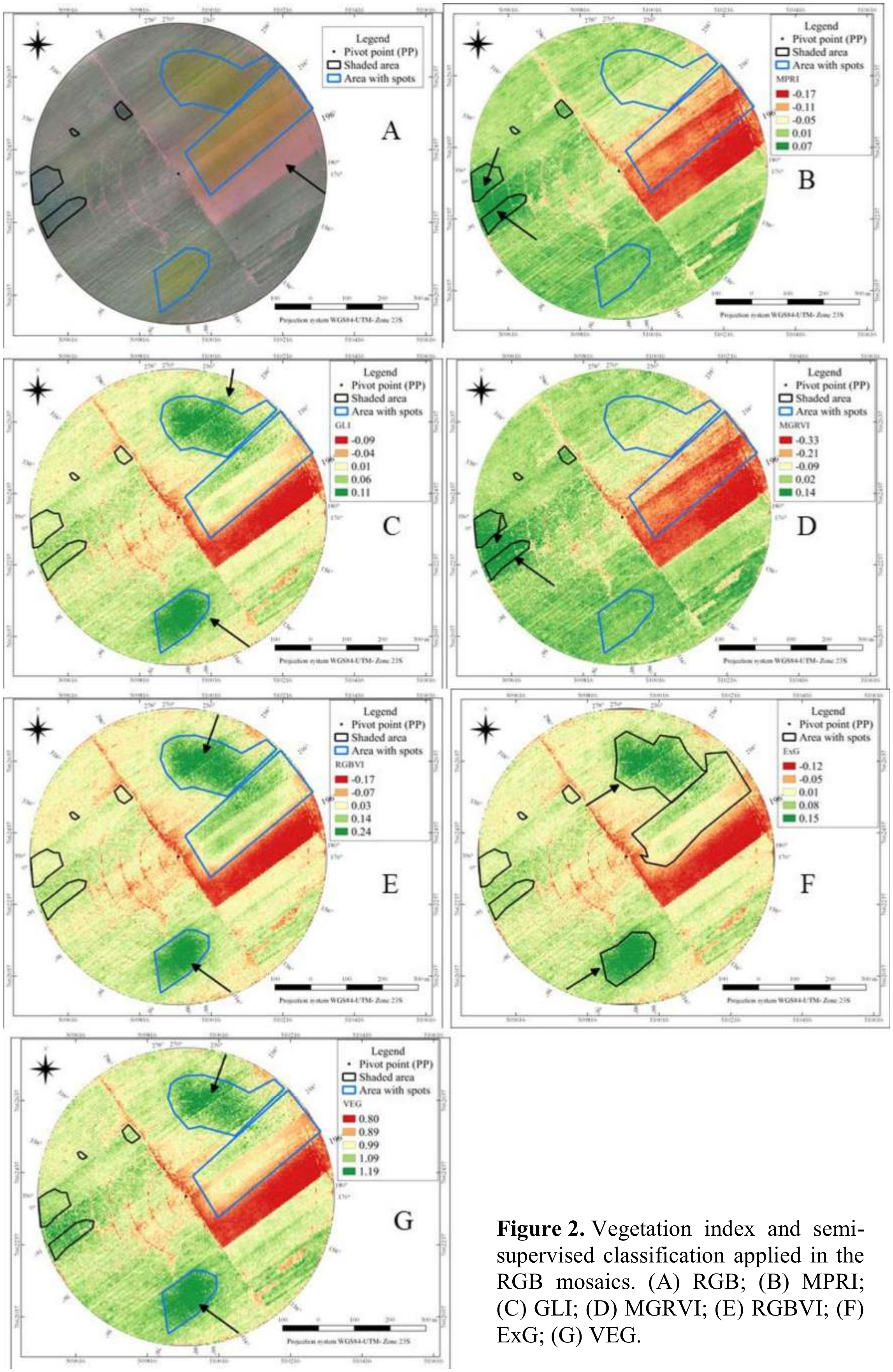

Figure 2. Vegetation index and semi-supervised classification applied in the RGB mosaics. (A) RGB; (B) MPRI; (C) GLI; (D) MGRVI; (E) RGBVI; (F) ExG; (G) VEG.

Bending et al. (2015) indicate that this VI is more efficient in the initial stages of development of the culture. Barret et al. (2015) found that RGBVI was highly correlated with NDVI, which is the VI most used in the research, and these authors emphasize that pasture monitoring can be performed with an aerial platform (eg an RPA) and an RGB camera. However, it is noteworthy that few studies have investigated the effects of light variations on RGB images obtained by APRs and their effects on the decision process.

In this study the IV ExG (Fig. 2, F) in comparison as Fig. 2, A and MPRI (Fig. 2, B) was not able to distinguish vegetation (represented by green coloration) of soil (represented by red color) effectively, indicating a vegetation less dense (which is represented by a color lighter, with values close to 0.01). In the areas indicated by arrows indicating in Fig. 2, F a dark green coloration is observed, this fact is due to the fact that ExG classified this region as being an area with vegetation in a greater stage of development, which is not proven in the field and by Fig. 1, A. Such behavior is due to the presence of noises (yellow spots in Fig. 2, A).

Torrez-Sánchez et al. (2015) evaluated the effectiveness of vegetation segmentation using ExG VI with automatic classification methods, and the results reached an accuracy of approximately 90%, indicating an additional possibility for the use of this IV. The divergence between the result obtained by the authors and that of this study may be associated with the lack of ideal lighting conditions at the time of images collection, however, it is necessary to study more about which parameters cause greater influence in this type of IV.

VEG VI (Fig. 2, G) was able to enhance vegetation and soil exposed vegetation; however, this VI was also affected by areas with spots (indicated by the arrows in Fig. 2, G), as well as the ExG and RGBVI. Therefore, this VI should also be used with caution in agricultural monitoring, where there are significant variations in lighting conditions.

CONCLUSIONS

All of the evaluated VIs were affected by the variability in the lighting conditions at the site. The MPRI and MGRVI provided the best results in a qualitative assessment of the discrimination between vegetation and soil, but their use in images containing regions affected by shading should be evaluated carefully.

ACKNOWLEDGMENTS. We thank Itograss Agrícola, the Brazilian Federal Agency for Support and Evaluation of Graduate Education (CAPES), the National Council for Scientific and Technological Development (CNPQ), the Federal University of Lavras (UFLA), and the UFLA Office of Graduate Studies (PPGEA-UFLA) for their support in the development and presentation of this study.

REFERENCES

Bannari, A., Morin, D., Bonn, F. & Huete, A.R. 2009. A review of vegetation indices. *Remote sensing reviews*, 13(1–2), 95–120.

Bareth, G., Bolten, A., Hollberg, J., Aasen, H., Burkart, A. & Schellberg, J. 2015. Feasibility study of using non-calibrated UAV-based RGB imagery for grassland monitoring: case study at the Rengen Long-term Grassland Experiment (RGE), Germany. *DGPF Tagungsband*, **24**, pp. 1–7.

Barrero, O. & Perdomo, S.A. 2018. RGB and multispectral UAV image fusion for Gramineae weed detection in rice fields. *Precision Agriculture* **19**(5), 809–822.

Bendig, J., Yu, K., Aasen, H., Bolten, A., Bennertz, S., Broscheit, J. & Bareth, G. 2015. Combining UAV-based plant height from crop surface models, visible, and near infrared vegetation indices for biomass monitoring in barley. *International Journal of Applied Earth Observation and Geoinformation* **39**, pp. 79–87.

de Godoy, L.J.G., Bôas, R.L.V. & Backes, C. 2012. Production of Saint Augustine grass carpets submitted to nitrogen doses. *Semina: Ciências Agrárias* **33**(5), 1703–1716.

Feng, Q., Liu, J. & Gong, J. 2015. UAV remote sensing for urban vegetation mapping using random forest and texture analysis. *Remote Sensing* **7**(1), 1074–1094.

Hamuda, E., Glavin, M. & Jones, E. 2016. A survey of image processing techniques for plant extraction and segmentation in the field. *Computers and Electronics in Agriculture* **125**, 184–199.

Hunt, E.R., Cavigelli, M., Daughtry, C.S., Mcmurtrey, J.E. & Walthall, C.L. 2005. Evaluation of digital photography from model aircraft for remote sensing of crop biomass and nitrogen status. *Precision Agriculture* **6**(4), 359–378.

Kakaes, K., Greenword, F., Lippincott, M., Dosemagen, S., Meier, P. & Wich, S.A. 2015. Drones and Aerial Observation: New Technologies for Property Rights. Human Rights, and Global Development: *A Primer (New America*, *2015*), 514–519.

Kazmi, W., Garcia-Ruiz, F.J., Nielsen, J., Rasmussen, J. & Andersen, H.J. 2015. Detecting creeping thistle in sugar beet fields using vegetation indices. *Computers and Electronics in Agriculture* **112**, 10–19.

Liu, C., Sun, P.S. & Liu, S.R. 2016. A review of plant spectral reflectance response to water physiological changes. *Chinese Journal of Plant Ecology* **40**, 80–91.

Louhaichi, M., Borman, M.M. & Johnson, D.E. 2001. Spatially Located Platform and Aerial Photography for Documentation of Grazing Impacts on Wheat. *Geocarto International* **16**(1), 65–70.

Meyer, G.E. & Neto, J.C. 2008. Verification of color vegetation indices for automated crop imaging applications. *Computers and electronics in agriculture* **63**(2), 282–293.

Ortega-TeroL, D., Hernandez-Lopez, D., Ballesteros, R. & Gonzalez-Aguilera, D. 2017. Automatic Hotspot and Sun Glint Detection in UAV Multispectral Images. *Sensors* **17**(10). 2352.

Ponti, M.P. Segmentation of low-cost remote sensing images combining vegetation indices and mean shift. *IEEE Geoscience and Remote Sensing Letters* **10**(1), pp. 67–70.

Rasmussen, J., Ntakos, G., Nielsen, J., Svensgaard, J., Poulsen, R.N. & Christensen, S. 2016. Are vegetation indices derived from consumer-grade cameras mounted on UAVs sufficiently reliable for assessing experimental plots?. *European Journal of Agronomy* 74, 75–92.

Romeo, J., Pajares, G., Montalvo, M., Guerrero, J. M., Guijarro, M. & de la Cruz, J.M. 2013. A new Expert System for greenness identification in agricultural images. *Expert Systems with Applications* **40**(6), 2275–2286.

Torres-Sánchez, J., López-Granados, F. & Peña, J.M. 2015. An automatic object-based method for optimal thresholding in UAV images: Application for vegetation detection in herbaceous crops. *Computers and Electronics in Agriculture* **114**. 43–52.

Vega, F.A., Ramírez, F.C., Saiz, M.P. & Rosúa, F.O. 2015. Multi-temporal imaging using an unmanned aerial vehicle for monitoring a sunflower crop. Biosystems Engineering 132, 19–27.

Vergara-Díaz, O., Zaman-Allah, M.A., Masuka, B., Hornero, A., Zarco-Tejada, P., Prasanna, B.M., ... & Araus, J.L. 2016. A novel remote sensing approach for prediction of maize yield under different conditions of nitrogen fertilization. *Frontiers in plant science 7*, 666.

Woebbecke, D.M., Meyer, G.E., Von Bargen, K. & Mortensen, D.A. 1995. Color indices for weed identification under various soil, residue, and lighting conditions. *Transactions of the ASAE* **38**(1), 259–269.

Xiang, H. & Tian, L. 2011. Development of a low-cost agricultural remote sensing system based on an autonomous unmanned aerial vehicle (UAV). *Biosystems engineering* **108**(2), 174–190.

Xiao, J.,& Moody, A. 2005. A comparison of methods for estimating fractional green vegetation cover within a desert-to-upland transition zone in central New Mexico, USA. *Remote sensing of environment* **98**(2-3), 237–250.

Yang, Z., Willis, P. & Mueller, R. 2008. Impact of band-ratio enhanced AWIFS image to crop classification accuracy. *Pecora* **17**, 18–20.

Zhang, J., Yang, C., Song, H., Hoffmann, W.C., Zhang, D. & Zhang, G. 2016. Evaluation of an airborne remote sensing platform consisting of two consumer-grade cameras for crop identification. *Remote Sensing* **8**(3), 257.

Zhang, C. & Kovacs, J.M. 2012. The application of small unmanned aerial systems for precision agriculture: a review. *Precision agriculture* **13**(6), 693–712.